

Bright X-ray source populations in the starburst galaxies NGC 4038/4039

Xi-Wei Liu and Xiang-Dong Li

Astronomy Department, Nanjing University, Nanjing, 210093, China

Received ; accepted

Abstract Assuming a naive star formation history, we construct the synthetic X-ray source populations for comparison with the X-ray luminosity function (XLF) of the interacting galaxies NGC 4038/4039 using a population synthesis code. We have considered high- and intermediate-mass X-ray binaries, young rotation-powered pulsars and fallback disc-fed black holes in modelling the bright X-ray sources detected. To examine the effects of the input parameters on the calculated results we produce a series of hybrid models. We find that for typical binary evolution parameters, it is difficult to match the observed XLF shape, and the predicted XLFs seem to be steeper than those of starburst and late type spiral galaxies. We note that the shape of the XLFs depends critically on the existence of XLF break for young populations, which seems to be a popular feature in theoretical population synthesis works. We discuss possible reasons and implications on the discrepancy of the calculated and observational XLFs.

Key words: binaries: close — galaxies: individual (NGC 4038/4039) — stars: evolution — X-ray: binaries

1 INTRODUCTION

With *Chandra*'s unprecedent sensitivity and angular resolution, populations of individual X-ray sources, with luminosities comparable to those of Galactic X-ray binaries, can be detected at the distance of the Virgo Cluster and beyond (Fabbiano 2006). *Chandra* observations of the merging galaxies NGC 4038/4039 (the Antennae) provide a unique opportunity for the study of the X-ray source populations in young and intense starburst environments (Fabbiano, Zezas & Murray 2001; Zezas et al. 2002a, 2002b; Zezas &

* E-mail: liuxw@nju.edu.cn, lixd@nju.edu.cn

Fabbiano 2002, hereafter ZF02). Among the 43 point-like sources detected by *Chandra* (down to a limiting luminosity of $\sim 10^{38}$ erg s $^{-1}$), 17 have (isotropic) X-ray luminosities significantly in excess of the Eddington limit of stellar-mass black holes (BHs), and are classified as Ultraluminous X-ray sources (ULXs). Although accretion binaries with a BH of mass in the range $100 - 1000M_{\odot}$ (i.e., intermediate mass black holes, IMBHs) can easily explain these super-Eddington luminosities, they may not account for the majority of the ULXs in the Antennae galaxies (ZF02). One possible explanation is that the X-ray radiation of the ULXs is not isotropic, so the real luminosities are lower by a factor of $\sim 10 - 100$ (King et al. 2001). Alternatively, Begelman (2002) suggested that in radiation-dominated accretion disks, the radiation could escape from the disk (due to the “photon bubble instability”) at a rate higher than predicted by the standard accretion disk theory, so that the escaping flux could exceed the Eddington luminosity by a factor of up to $\sim 10 - 100$. ZF02 derived the X-ray luminosity function (XLF) of the X-ray source populations in the Antennae. The cumulative XLF is well fit with a power-law with an index of $\alpha = -0.45$, which is consistent with (though slightly flatter than) the slope of the “universal luminosity function” for the HMXB populations in various types of galaxies (Grimm, Gilfanov & Sunyaev 2003). In this paper we try to reproduce the observed XLF (with both the shape and the absolute source number) by using evolutionary population synthesis (EPS) method, and to evaluate the effects of the input parameters on the calculated results. Although there have been many observations of the point X-ray sources in external galaxies, theoretical investigations on the X-ray source populations remain to be limited. A similar population synthesis study on the XLF of NGC 1569 has been done by Belczynski et al. (2004). However, they did not try to fit the absolute number of the detected X-ray sources in this dwarf irregular galaxy, and only X-ray binary populations were taken into account. In §2 We describe the population synthesis method and the models for various types of X-ray sources. The calculated results are presented in §3. Discussion and conclusions are in §4.

2 MODEL DESCRIPTION

2.1 Method and input parameters

We use the EPS code developed by Hurley, Pols & Tout (2000) and Hurley, Tout & Pols (2002, hereafter HTP02) to calculate the expected numbers and X-ray luminosity distributions in the Antennae for various types of single and binary X-ray source populations. This code incorporates the evolution of single stars with binary star interactions, such as mass transfer, mass accretion, common-envelope (CE) evolution, collisions, supernova (SN) kicks, tidal friction and angular momentum loss mechanisms (i.e. mass loss, magnetic braking and gravitational radiation). In this work, we have modified the EPS code in the following aspects to perform better in simulating binary evolution in a

variety of circumstances. Firstly, the original EPS code produces BHs with unreasonable low masses. In Fig. 1 we show the masses of the stellar remnants (i.e. the compact objects) as a function of the masses of their zero-age main sequence (ZAMS) stars. The BH masses are determined by an empirical function of the Carbon-Oxygen core masses of the pre-collapse progenitor stars, i.e. $m_{\text{BH}} = 1.17 + 0.09m_{\text{co}}$. In the top panel of Fig. 1 we show the calculated results with the original code. It is shown that the natal BH masses are in a narrow range of $\sim 1.8 - 2.0 M_{\odot}$, which are significantly smaller than those ($\sim 3 - 18 M_{\odot}$) of the observed BH candidates in our Galaxy (Remillard & McClintock 2006). We have modified the empirical formula in the code to be $m_{\text{BH}} = -33 + 6m_{\text{co}}$, so that a larger range of BH masses ($\sim 4 - 10 M_{\odot}$ and $\sim 5 - 26 M_{\odot}$ for population I and II stars respectively) can be produced, which are shown in the middle and lower panels. The figure illustrates that the lower limits for the BH progenitor masses are $\sim 23 M_{\odot}$ ($Z = 0.02$) and $\sim 20 M_{\odot}$ ($Z = 0.001$), consistent with the putative values (e.g. Fryer 1999). It is noted that a similar modification has been done by Belczynski, Sadowski & Rasio (2004).

Secondly, the EPS code assumes that all non-compact stars suffer magnetic braking if it is more massive than $0.35 M_{\odot}$. However, stars more massive than $1.5 M_{\odot}$ have radiative envelopes which cannot generate strong magnetic field. So we taken into account the magnetic braking mechanism only for stars of $M < 1.5 M_{\odot}$. Thirdly, when a main sequence star overfills its Roche lobe and is 2.5 times more massive than its companion (the accretor), a very rapid, dynamically unstable mass transfer phase would emerge, and the orbital separation would decline dramatically. We thus assume the binary would coalescence, and no further calculation is taken.

The fourth modification is about the natal BH kick velocities. During the SN explosions, a kick velocity v_{k} is imparted on the newborn compact stars with the Maxwellian distribution

$$P(v_{\text{k}}) = \sqrt{\frac{2}{\pi}} \frac{v_{\text{k}}^2}{\sigma^3} \exp\left(-\frac{v_{\text{k}}^2}{2\sigma^2}\right) \quad (1)$$

where $\sigma = 265 \text{ km s}^{-1}$ for neutron stars (NSs) (Hobbs et al. 2005). We assume that only those BHs experienced SN explosions would be imparted on a natal kick velocity, which is inversely proportional to the BH mass, i.e. $v_{\text{kick},\text{BH}} = 1.4/M_{\text{BH}} \times v_{\text{kick},\text{NS}}$. Apart from core collapse SNe, Belczynski & Taam (2004) suggested the formation of NSs via accretion-induced collapse of massive white dwarfs (WDs). We do not take it into account due to the large uncertainties of the AIC assumption.

Now we move to the parameters input into the code for population synthesis. We assume a fraction f ($0 < f < 1$) of stars are born in binaries. Surveys of M dwarfs within 20 pc have suggested that f may be a function of stellar spectral types (Fischer & Marcy 1992). According to recent works on stellar multiplicity (Lada 2006; Kobulnicky, Fryer & Kiminki 2006, hereafter KFK06), stars with later spectral types are more likely

single, for example, $f > 50\%$ for G stars, and $f > 0.6$ (in the most probable range $0.7 < f < 0.85$) for massive O/B stars in the Cygnus OB2 association surveyed by KFK06. We have adopted $f = 0.5$ or 0.8 in our calculations. The initial mass function (IMF) of Kroupa, Tout, & Gilmore (1993) is taken for the primary's mass (M_1) distribution. For the secondary stars (of mass M_2), in our standard model we assume uniform distributions of the mass ratio $q = M_2/M_1$ between 0 and 1 and of the logarithm of the orbital separation $\ln a$. However, KFK06 suggested more general power-law distributions of the secondary masses and orbital separations, i.e., $P(q) \propto q^\alpha$ and $P(\ln a) \propto (\ln a)^\beta$, where the power-law indices $\alpha > 0$ and $-2 < \beta < 0.5$. We have designed several models to examine the effects of the changes of these primordial binary parameters (f , α and β) on the results (see next section).

Reasonable estimates of the star formation rate (SFR) and star formation history (SFH) are crucial to population synthesis of the X-ray sources detected in the Antennae galaxies. For the SFR we adopt the value of $7.1 M_\odot \text{yr}^{-1}$ for stars more massive than $5 M_\odot$ (Grimm, Gilfanov & Sunyaev 2003), which was obtained based on the measurement of several canonical indicators of SFR, namely UV, H α , FIR and thermal radio emission fluxes. This values was then converted into the specific SFRs S_s and S_b used in the EPS code. Here S_s and S_b (in unit of yr^{-1}) denote the formation rates of single and binary star populations, respectively. Since the binary fraction is f , we have

$$\frac{2S_b}{S_s + 2S_b} = f. \quad (2)$$

The amount of the mass produced per year in the stars more massive than $5 M_\odot$ is

$$S_b \int_5^\infty m_1 \xi(m_1) dm_1 + S_b \int_5^\infty \xi(m_1) \left(\int_5^{m_1} \frac{m_2}{m_1} dm_2 \right) dm_1 + S_s \int_5^\infty m \xi(m) dm = 7.1, \quad (3)$$

where $\xi(m)$ is the IMF. The fist and second terms on the left-hand-side of Eq. (3) represent the amount of mass formed per year as the primary and secondary star of a binary, respectively. Those formed in single stars is evaluated in the third term. Combining Eqs. (2) and (3), we have

$$S_s = \frac{14.2 - 14.2f}{0.144 - 0.045f} \text{ and } S_b = \frac{7.1f}{0.144 - 0.045f} \quad (4)$$

The values of the single and binary star SFRs can be input into the single stellar evolution (SSE) and binary stellar evolution (BSE) code, respectively (see §4.1 of HTP02 for details). For a binary fraction $f = 0.5$, we get $S_s = 58.4 \text{yr}^{-1}$ and $S_b = 29.2 \text{yr}^{-1}$. According to the most common models on the evolution of the Antennae, closest passage of the two galaxies comprising the Antennae happened roughly 200 Myrs ago (Barnes 1988; Mihos, Bothun & Richstone 1993). The merging induced star formation tends to persist for 0.5 to 1 dynamical time (i.e., the orbital time-scale of the last encounter) (Mengel et al. 2005). It is expected that most of the X-ray sources detected are relatively young objects produced after the merging process, so we adopt a naive model for the

SFH that assumes the Antennae galaxies have been keeping the current SFR for the last 300 or 100 Myr. Since we are concerned with young populations, we do not take the SFH earlier into account.

2.2 Models for X-ray sources

We consider three types of X-ray source populations for the X-ray sources detected in the Antennae.

A large fraction of the X-ray sources should be X-ray binaries containing accreting NSs or BHs. For starburst galaxies like the Antennae, high-mass X-ray binaries (HMXBs) with the secondary masses $M_2 > 8 M_\odot$ and intermediate-mass X-ray binaries (IMXBs) with $2 M_\odot < M_2 < 8 M_\odot$ are the most natural explanation for the bright point-like sources in these galaxies (low-mass X-ray binaries are too old for our assumed SFH). According to the manner of the accretion onto the accretor (NSs or BHs), X-ray binaries can be divided into two classes, wind-accreting (WA) and Roche-lobe overflow (RLOF) systems. In the former case we adopt the standard Bondi & Hoyle (1944) wind-accretion formula to calculate the mass accretion rate of the NSs/BHs. The velocity v_W of the winds from the massive donor stars is taken to be $v_W = \sqrt{2\beta(GM_2/R_2)}$, where R_2 is the radius of the donor star, and the value of β depends on the spectral type of the stars. HTP02 suggested it is in the range of 0.125 – 7.0. The gravitational energy released by the accreted material is converted into radiation, and we have to correct the calculated bolometric luminosities into those in the *Chandra* detection band of 0.1 – 10 keV. Since the WA NS systems have relatively hard spectra that can be described with a $\Gamma \sim 0$ power law below 10 keV (e.g. Campana et al. 2001), we assume that almost all the radiation energy is concentrated in the *Chandra* band, and no bolometric correction is needed. For all the other X-ray binaries we adopt a correction factor of 0.2.

Current stellar evolution models predict that during the core collapse of massive stars, a considerable amount of the stellar material will fall back onto the compact, collapsed remnants (NSs or BHs), usually in the form of an accretion disc. Li (2003) suggested that some of the ULXs in nearby galaxies, which are associated with supernova remnants, may be BHs accreting from their fallback discs. Not all natal BHs can possess a fallback disc, unless the BH progenitors have enough angular momentum to form a centrifugally supported disc. The condition that matter does not spiral into the BH at the onset of collapse is that the rotational energy of the matter should be greater than half the gravitational potential energy (Izzard, Ramirez-Ruiz & Tout 2004): $J^2/(2I) \geq GM_{BH}m/(2r_{LSO})$, where J is the angular momentum of the matter, $I = mr_{LSO}^2$ is its moment of inertia and r_{LSO} is the radius of the last stable orbit (LSO) around a BH. In fact for the Population I ($Z = 0.02$) stars, from our calculations only those in close binaries can be spun up so fast (due to spin-orbit tidal evolution) that fallback discs

can form after core collapse. After an initial transient phase of duration, the disc mass M_d , outer radius R_d , and mass accretion rate \dot{M}_d obey the simple power-law evolution, i.e. $M_d \propto t^{-p}$, $R_d \propto t^{2p}$ and $\dot{M}_d \propto t^{-(1+p)}$ (Cannizzo, Lee & Goodman 1990), and we adopt $p = 3/16$ in this paper. Menou, Perna & Hernquist (2001, hereafter MPH01) argued that the power-law evolution breaks down when the disc is cool enough to become neutral. We thus limit our calculation on the disc evolution to the neutralization time t_n . Following MPH01 we derived the time t_n in the cases of non-irradiated and irradiated discs, respectively

$$t_n = R_8(t_0)^{\frac{7p-6}{2+14p}} \cdot 6.6 \times 10^{\frac{12-35p}{1+7p}} \left[\frac{M(t_0)}{\eta \cdot 10^{-3} M_\odot} \right]^{\frac{1}{1+7p}} T_{c,6}^{-\frac{7p}{1+7p}} \text{ yr}, \quad (5)$$

$$t_n^{\text{irr}} = R_8(t_0)^{\frac{5p-4}{2+10p}} \cdot 6.6 \times 10^{\frac{11-25p}{1+5p}} \left[\frac{M(t_0)}{\eta \cdot 10^{-3} M_\odot} \right]^{\frac{1}{1+5p}} T_{c,6}^{-\frac{5p}{1+5p}} \text{ yr}, \quad (6)$$

where $R_8(t_0)$ is the initial radius of the disc in units of 10^8 cm, $T_{c,6}$ the typical temperature of the disc during the initial transient phase in units of 10^6 K, M_{t_0} the initial mass of the disc, and η includes all other uncertainties. Here we adopt $R_8(t_0) = 1$, $T_{c,6} = 1$ and $\eta = 1$. For $M(t_0)$ we assume a uniform distribution of $\log M(t_0)$ in the range of $10^{-5} - 1 M_\odot$. The bolometric correction factor of the fallback disc is also chosen to be 0.2.

Moreover, the X-ray emission from accreting compact stars (both single and in binaries) is generally assumed to be isotropic. However, for disc accreting sources, the geometric effect may affect the apparent luminosity distributions (Zhang, 2005). For the RLOF X-ray binaries and the fallback disc-fed BHs we have taken into account the geometric effect in calculating their X-ray luminosities (see §2.2 of Liu & Li 2006 for details).

Young pulsars are also X-ray emitters. There appears to be a strong correlation between the rates of rotational energy loss \dot{E} and their X-ray luminosities L_X (Seward & Wang 1988; Becker & Trumper 1997 and Possenti et al. 2002). Perna & Stella (2004) argued that a fraction of ULXs could be young, Crab-like pulsars, the X-ray luminosities of which are powered by rotation. Especially they noted that starburst galaxies should each have several of these sources and that the X-ray luminosity of a few percent of galaxies is dominated by a single bright pulsar with $L_X \geq 10^{39}$ ergs $^{-1}$, roughly independently of its SFR. Following Perna & Stella (2004) and Liu & Li (2006) we adopt the empirical relation by Possenti et al. (2002) to estimate the 2 – 10 kev X-ray luminosities of pulsars.

To our knowledge this work is the first to include all the three types of X-ray source populations suggested in the literature in modeling the XLF of external galaxies.

3 RESULTS

We have adopted a variety of models with different assumptions for the input parameters (see Table 1). We set Model 1 (hereafter M1) as the “standard model”, while other models are designed to test the effects of the input parameters by changing one by one of them.

In Fig. 2 we show the calculated XLFs in model M1 of HMXBs, IMXBs, fallback disc sources, pulsars and the total X-ray sources in the Antennae galaxies. One can see that IMXBs dominate the total X-ray luminosity range, and young pulsars also contribute considerably to the brightest sources. HMXBs play a minor role in the bright X-ray sources due to their relatively short lifetime compared to IMXBs. Fallback disc sources are much fewer than the above three classes of sources.

The XLFs (or the components of them) change with the input parameters, as shown in Figs. 3 and 4. In order to evaluate the effect of the uncertainty of the SFH, we show the differences of the XLFs of NS/BH RLOF systems in IMXBs between models M1 and M2 (in which the SFH was decreased from 300 Myr to 100 Myr) in panel (a) of Fig. 3. Obviously, longer SFH leads to greater number of X-ray binaries. Actually, in some cases it takes the primordial binaries more than 100 Myr to become IMXBs. Here we present an example to show how a typical RLOF NS IMXB system forms. Let us consider a binary consisting of a $9.19 M_{\odot}$ primary and a $3.62 M_{\odot}$ secondary in a 2.297 yr orbit. About 32 Myr later, the primary star evolves to the AGB stage and fill its Roche lobe when the orbital period is 2.078 yr. Because the mass ratio $8.72/3.71 > q_{\text{crit}}$, where q_{crit} (~ 0.8 for GB and AGB stars) is the critical mass ratio above which mass transfer is dynamically unstable, a CE forms, and the orbital period decreases dramatically to 2.98 days within a very short time. After the CE phase the binary is composed of a naked helium star (of mass $2.58 M_{\odot}$), the helium core of the primary, and the secondary star with mass hardly changed. Around 0.12 Myr later the helium star collapses to a $1.3 M_{\odot}$ NS (accompanied by a Ib SN explosion), the orbital period increases to 29.9 days with an eccentricity ~ 0.6 . Meanwhile, the mass of the secondary star grows to $4.22 M_{\odot}$ due to accretion from the strong winds from the helium star. The subsequent binary evolution is governed by the nuclear evolution of the secondary star, which expands along with orbital shrink. Thus the orbital period decreases from 29.9 to 12.6 days when the secondary evolves to the Hertzsprung gap and fills its Roche lobe to transfer mass to the NS. It is now can we observe this system as a NS RLOF X-ray binary. In 0.02 Myr the binary becomes luminous enough ($> 10^{36} \text{ erg s}^{-1}$) to be counted in our XLF. The duration from the ZAMS to the begining of the luminous X-ray binary phase is 168.9 Myr, which exceeds the 100 Myr SFH of model M2.

In panel (b) we show the effect of binary fraction f on the XLF of rotation-powered pulsars, which changes from 0.5 in M1 to 0.8 in M3. Pulsars in binaries are less than single pulsars in M1. This is easily understood. In binaries the secondary stars are always less massive than the primary star, so the former has less possibility to evolve to NSs than the latter. Since we assume the same IMF for the primary stars as that for the single stars, less pulsars in binaries are then produced. When we change the binary fraction from 0.5 to 0.8, however, binary pulsars become to dominate.

We also compare the XLFs of BH IMXBs in panels (c) and (d) of Fig. 3 for different choices of q and $\ln a$ distributions. There will be less RLOF X-ray binaries when the secondary stars are biased to more massive stars, or in small initial orbits. This feature will be discussed later.

In panel (a) of Fig. 4 we show the XLFs of luminous fallback discs with and without considering the irradiation effect. The irradiation, as an extra source of heating, is able to keep the disc ionized, postponing the moment when the disc becomes neutral with more luminous disc sources expected.

The CE efficiency parameter α_{CE} plays an important role in the formation of various kinds of close binaries (e.g. LMXBs, IMXBs and HMXBs). To see the dependence of the results on α_{CE} , we compare the XLFs of NS IMXBs in model M1 ($\alpha_{CE} = 1.0$) with those of models M8 ($\alpha_{CE} = 2.0$) and M9 ($\alpha_{CE} = 0.1$) in panel (b) of Fig. 4. Note that $\alpha_{CE} = 2.0$, which seems to violate the conversion of energy, is required to explain the existence of wide binary millisecond pulsars (e.g. van den Heuvel 1994). But more recent investigations seem to favor smaller value of α_{CE} (Dewi & Tauris 2000). Figure 4b illustrates that the number of NS IMXBs decreases with decreasing α_{CE} , since the binary would be more likely to coalesces with low efficiency of the CE ejection when the primary evolves to the AGB stage to overflow its Roche-lobe.

The effect of the allowed super-Eddington accretion limit on the XLFs is shown in panel (c). Obviously, release the limit from 10 (in M1) to 100 (in M11) would produce more bright X-ray sources, and make the high luminosity end of the XLFs flatter. This is helpful for simulating the flat XLFs of young populations (see below).

The number of luminous WA systems is sensitive to the value of β as seen in panel (d). According to the Bondi & Hoyle (1944) mechanism, the small β , the high the accretion rate, and hence more luminous sources. When β changes from 0.5 (in M1) to 1 (in M7), the numbers of bright WA HMXBs and IMXBs decreases by a factor of 2 and by 10%, respectively.

We also construct model M10 (with $Z = 0.001$) to evaluate how metallicity affects the results. Lower metallicity would significantly increase the numbers of all kinds of luminous X-ray sources, in particular the number of fallback disc sources. The main reason is that stars with lower metallicity have lower wind mass loss, hence lower masses of the NS or BH primaries are required. Additionally, lower mass-loss also means lower angular momentum loss from either the binary orbits or the stellar rotation, leading to faster spins of the pre-collapse progenitors of BHs, and higher possibility for the formation of fallback discs. However, the total number of the X-ray sources more luminous than $10^{38} \text{ erg s}^{-1}$ in M10 is ~ 2000 (this is in major due to the great number of fallback disc sources produced in single stars, in contrast to the result in model M1 where the fallback disc sources are exclusively produced in binaries), about 50 times more than observed.

This suggests that most of the X-ray sources in the Antennae are not likely to descend from Population II stars.

We finally compare the calculated XLFs of 6 representative models (M1, M2, M5, M7, M9 and M12) with the observational one for the Antennae galaxies in Fig. 5. The latter can be fit with a power-law as $N(> L_X) = B (L_X/10^{38} \text{ erg s}^{-1})^{-\alpha}$, where $B = 38.9$ and $\alpha = 0.45$ (ZF02). This flat XLF is consistent with though slightly flatter than that of the so called *universal HMXB luminosity function* with $\alpha \sim 0.6$ deduced from a sample of nearby late-type/starburst galaxies observed with *Chandra* (Grimm, Gilfanov & Sunyaev 2003). The figure shows that none of the models except M12 are in acceptable agreement with the observational result - they usually overproduce sources with luminosities \sim a few $10^{37} - 10^{38} \text{ erg s}^{-1}$, while at the high luminosity end almost all the models underestimate the source number. We discuss the possible reasons and implications for this discrepancy in next section.

4 DISCUSSIONS

Zezas et al. (2002b) showed that the position of most of the Antennae sources is near but *not* coincident with optical young clusters (typical offsets are $\sim 100 - 300$ pc). Assuming that this displacement are caused by the motion due to supernova kicks, ZF02 constrained the nature of the X-ray sources, suggesting that they may be accreting NS/BH binaries with donor stars of masses ranging from 2 to $10 M_\odot$. This inference is consistent with our result that IMXBs dominate the XLF in the standard model M1 (see Fig. 2). However, the modeled XLF shows a clear break at a few $10^{38} \text{ erg s}^{-1}$, related to the Eddington luminosities of BHs. This makes the XLF steeper in the ULX luminosity range ($> 10^{39} \text{ erg s}^{-1}$) than the observational one, although the latter is subject to small number statistics and large error bars. There is evidence for the breaks in the luminosity functions for nearby galaxies (e.g. Sarazin et al. 2000; Shirey et al. 2001). However, the break luminosities are still uncertain because of the distance uncertainties.

Kilgard et al. (2002) show that the luminosity function slope is correlated with the age of the X-ray binary populations, and the luminosity functions of the starbursts are flatter than those of the spiral galaxies with relatively more sources at high luminosities. This is an reasonable idea, but their arguments are based on simplified assumption of single HMXB population as the X-ray sources detected. There is also no upper limit for the empirical luminosity distribution adopted.

Although there are obviously large uncertainties in the models for the X-ray source populations that can influence the final outcome, we note that the XLF breaks for young populations seem to be a general feature, and have already been predicted in other theoretical works (e.g. Fig. 1 of Belczynski et al. 2004; Fig. 6 of Rappaport et al. 2005). The shape of the XLF should be related to the NS/BH mass spectrum and the mass

transfer rates in binary stars (Grimm et al. 2003). The striking differences in the modeled and observational XLFs suggest that our understanding of the formation and radiation processes of the X-ray source populations is far from being complete. For example, the detected IMXBs and pulsars with $L_X < 10^{39}$ erg s $^{-1}$ may be fewer than expected. The existence of IMXBs have been long suggested (e.g. van den Heuvel 1975, Tauris & van den Heuvel 2003). Due to the relatively high mass ratio $M_{\text{donor}}/M_{\text{accretor}}$ (especially for NS accretors), the mass transfer occurs on a subthermal timescale (Tauris, van den Heuvel & Savonije 2000), and rapid mass loss is naturally expected. A large fraction of the X-rays are likely to be absorbed in the dense material surrounding the compact accretors or the binaries. Moreover, in our model for rotation-powered pulsars we employ the empirical relation between X-ray luminosities and the spin-down energy loss rates (\dot{E}) (eq.[7] in Liu & Li 2006). However, as noted by Possenti et al. (2002), there exists large scatter between the observational data and the fit relation. For instance, PSR J0537–6910 is one order of magnitude less luminous in X-rays than the Crab pulsar and PSR 0540–693 despite the similarity in the values of \dot{E} . Additionally, the X-ray emission of young pulsars can be attributed to magnetospheric processes, which is pulsed and intrinsically anisotropic. Thus the X-ray observation is subject to various geometrical corrections.

The best fit model M12 has several unusual features in the assumptions. First, the common envelope efficiency α_{CE} is set to be 0.1, much smaller than unity usually adopted. Second, the mass ratio q and orbital separation $\ln a$ distributions are taken to be q^1 and $(\ln a)^{-1}$ rather q^0 and $(\ln a)^1$ in M1. These factors can significantly decrease the number of IMXBs - the peculiar q and $\ln a$ distributions cause a bias toward the formation of narrow HMXBs, while small α_{CE} leads to coalescence of the progenitors of IMXBs. The resulting XLF does not show any prominent break since the dominant contribution has been taken by young pulsars and the fallback disc sources. This can be tested by future multi-wavelength observations. Third, the Eddington limit factor Edd was taken to be 100, so that the XLF can reach the brightest ULX luminosity range $\sim 10^{40}$ erg s $^{-1}$. It should be mentioned, however, that the assumption of Edd= 100 is highly uncertain and not verified. Alternatively, some of the ULXs in the Antennae galaxies could be IMBHs. Only a few these objects can account for the “overabundance” of the high luminosity end of the XLF. Currently our knowledge is unable to present stringent constraints on the nature and formation processes of these X-ray sources. More detailed X-ray luminosity function measurements of a large sample of galaxies across the full Hubble sequence are required to determine the nature of the break luminosities and the XLFs evolution. These observations, coupled with detailed stellar evolution models, should provide new insights into the compact object populations of external galaxies.

Acknowledgements We would like to thank Jarrod R. Hurley for kindly providing us his SSE and BSE codes and for valuable conversations. We thank Hai-Lang Dai, Wen-Cong Chen and Zhao-Yu Zuo for useful discussions. This work was supported by .

References

Barnes, J. E. 1988, *ApJ*, 331, 699
 Becker, W., & Trumper, J. 1997, *A&A*, 326, 682
 Begelman, M. C. 2002, *ApJ*, 568, L97
 Belczynski, K., Dalogera, A., Zezas, A. & Fabbiano, G. 2004, *ApJ*, 601, L147
 Belczynski, K. & Taam, R. E. 2004, *ApJ*, 616, 1159
 Belczynski, K., Sadowski, A., Rasio, F. A. 2004, *ApJ*, 611, 1068
 Bondi H., Hoyle F., 1944, *MNRAS*, 104, 273
 Cannizzo, J. K., Lee, H. M. & Goodman, J. 1990, *ApJ*, 351, 38
 Campana, S., Gastaldello, F., Stella, L., Israel, G. L., Colpi, M., Pizzolato, F., Orlandini, M., & Dal Fiume, D. 2001, *ApJ*, 561, 924
 Dewi, J.D.M & Tauris, T.M. 2000, *A&A*, 360, 1043
 Fabbiano, G. 2006, *ARA&A*, astro-ph/0511481
 Fabbiano, G., Zezas, A., & Murray, S. 2001, *ApJ*, 554, 1035
 Fischer, D. A. & Marcy, G. W. 1992, *ApJ*, 396, 178
 Fryer, C. L. 1999, *ApJ*, 522, 413
 Grimm, H.-J., Gilfanov, M., Sunyaev, R. 2003, *MNRAS*, 339, 793
 Gilgard, R. E. et al. 2002, *ApJ*, 573, 138
 Hobbs G., Lorimer D. R., Lyne A. G., & Kramer M. 2005, *MNRAS*, 360, 963
 Hurley, J. R., Pols, O. R. & Tout, C. A. 2000, *MNRAS*, 315, 543
 Hurley, J. R., Tout, C. A. & Pols, O. R. 2002, *MNRAS*, 329, 897
 Izzard, R. G., Ramirez-Ruiz, E., Tout, C. A. 2004, *MNRAS*, 348, 1215
 Kobulnicky, H. A., Fryer, C. L., Kiminki, D. C. 2006, submitted to *ApJ*, astro-ph/0605069
 Kroupa, P., Tout, C. A., & Gilmore, G., 1993, *MNRAS*, 262, 545
 Lada, C. J. 2006, *ApJ*, 640, L63
 Li, X. D. 2003, *ApJ*, 596, L199
 Liu, X. W. & Li, X. D. 2006, *A&A*, 449, 135, LL06
 Mengel, S., Lehnert, M. D., Thatte, N. & Genzel, R. 2005, *A&A*, 443, 41
 Menou, K., Perna, R. & Hernquist, L. 2001, *ApJ*, 559, 1032
 Mihos, J. C., Bothun, G. D. & Richstone, D. O. 1993, *ApJ*, 418, 82
 Perna, R. & Stella, L. 2004, *ApJ*, 615, 222
 Possenti, A., Cerutti, R., Colpi, M., & Mereghetti, S. 2002, *A&A*, 387, 993
 Rappaport, S. A., Podsiadlowski, Ph., & Pfahl, E. 2005, *MNRAS*, 356, 401
 Remillard, R. A., & McClintock, J. E. 2006, *ARA&A*, in press
 Sarazin, C. L., Irwin, J. A., & Bregman, J. N. 2000, *ApJ*, 544, L101
 Seward, F. D. & Wang, Z. 1988, *ApJ*, 332, 199
 Shirey, R., et al. 2001, *A&A*, 365, L195
 Tauris, T.M. & Dewi, J.D.M 2001, *A&A*, 369, 170
 Tauris, T. M. & E. P. J. van den Heuvel 2003, Review in the book 'Compact Stellar X-Ray Sources', eds. W.H.G. Lewin and M. van der Klis, Cambridge University Press, astro-ph/0303456
 Tauris, T. M., E. P. J. van den Heuvel & Savonije, G. J. 2000, *ApJ*, 530, L93
 van den Heuvel, E. P. J. 1975, *ApJ*, 198, L109
 van den Heuvel, E. P. J. 1994, *A&A*, 291, L39
 Zezas, A., Fabbiano, G., Rots, A. H. & Murray, S. S. 2002a, *ApJS*, 142, 239
 Zezas, A., Fabbiano, G., Rots, A. H. & Murray, S. S. 2002b, *ApJ*, 577, 710
 Zezas, A. & Fabbiano, G. 2002, *ApJ*, 577, 726, ZF02
 Zhang, S. N. 2005, *ApJ*, 618, L79

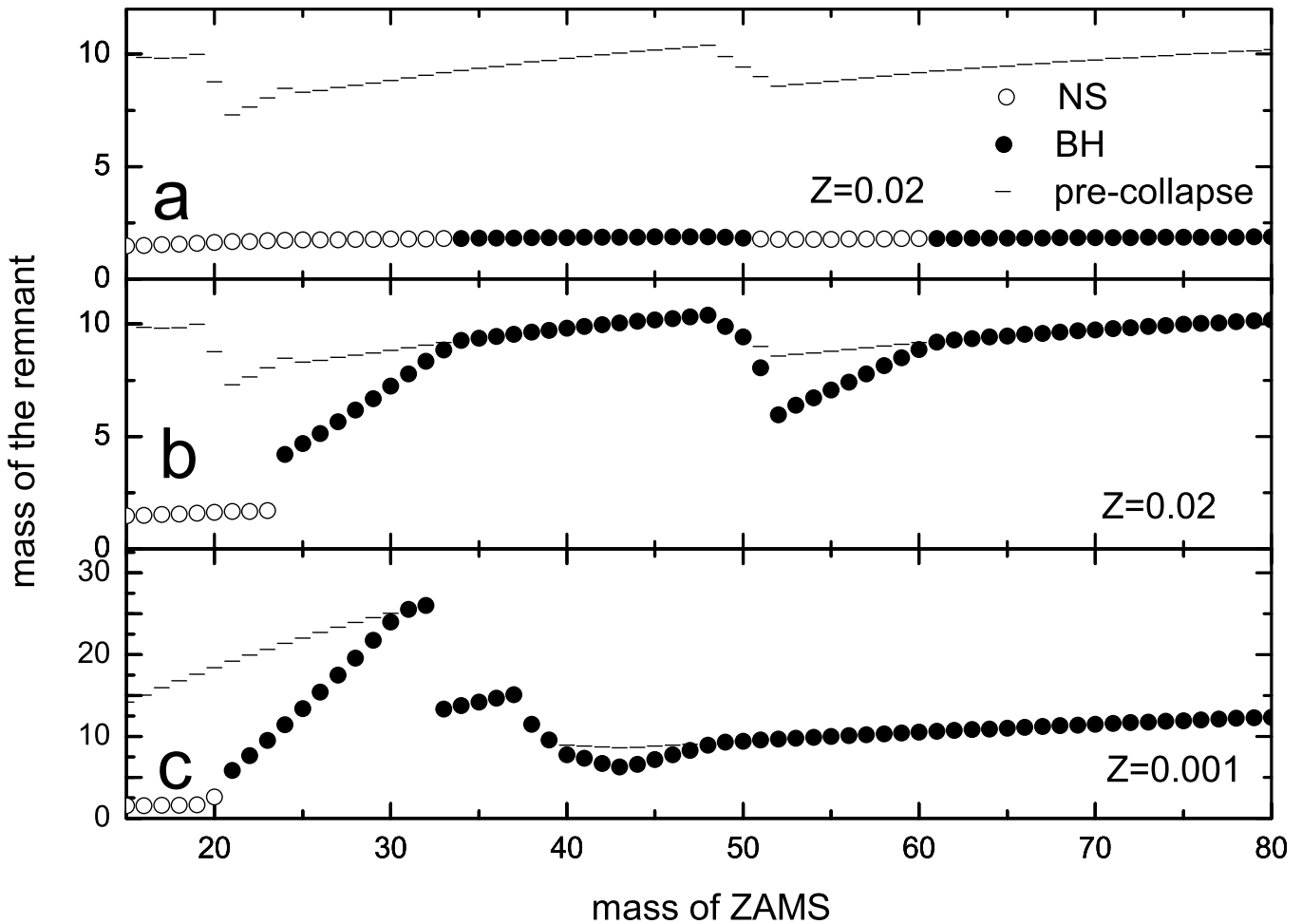


Fig. 1 Final remnant masses as a function of that of ZAMS progenitors for different metallicities. Top panel shows the result of the original BSE code, middle and bottom panels shows that of our modified code. Remnants of different types: NS and BH are marked.

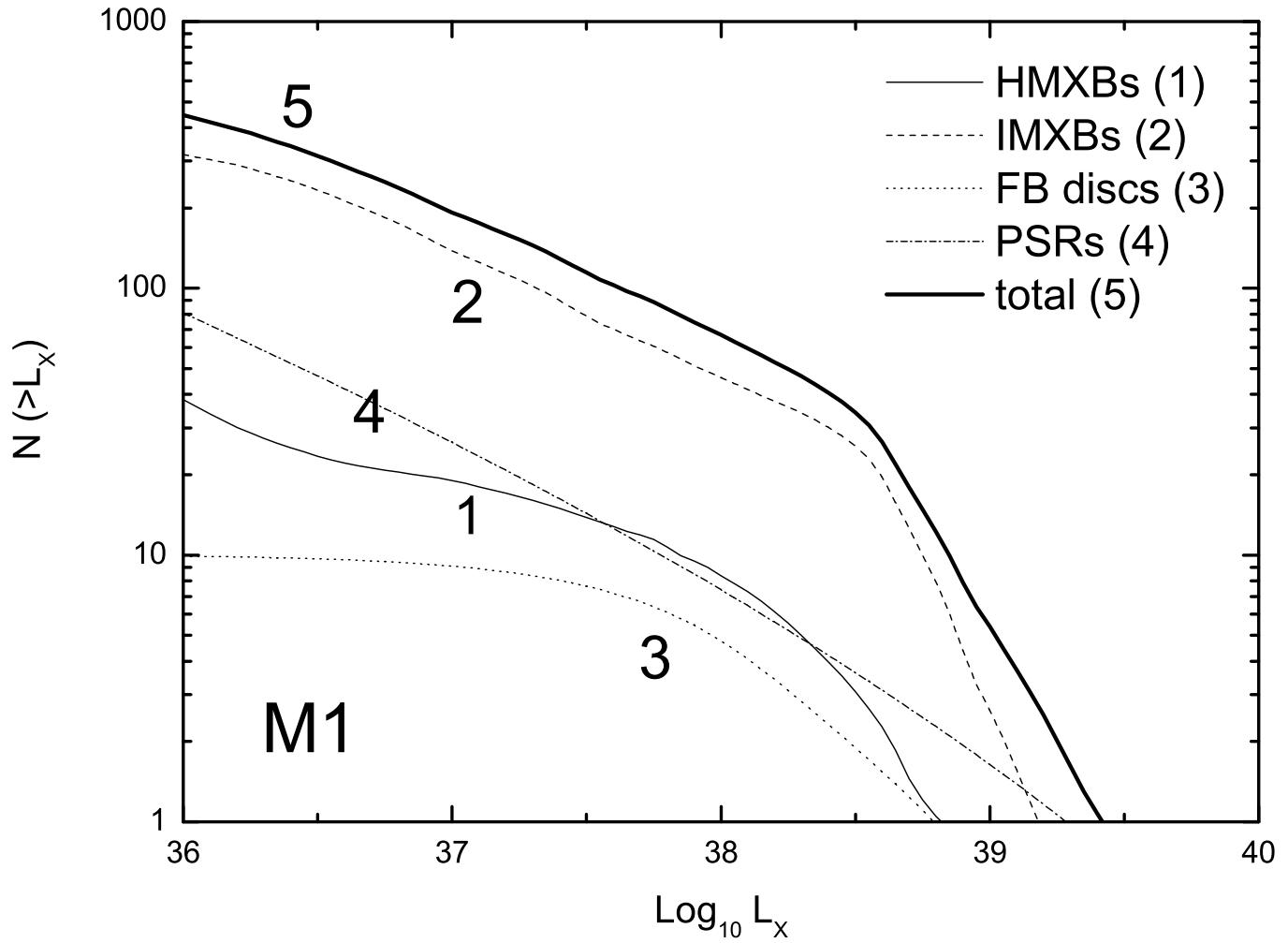


Fig. 2 The XLFs of model M1. For clarity we mark different lines with different numbers.

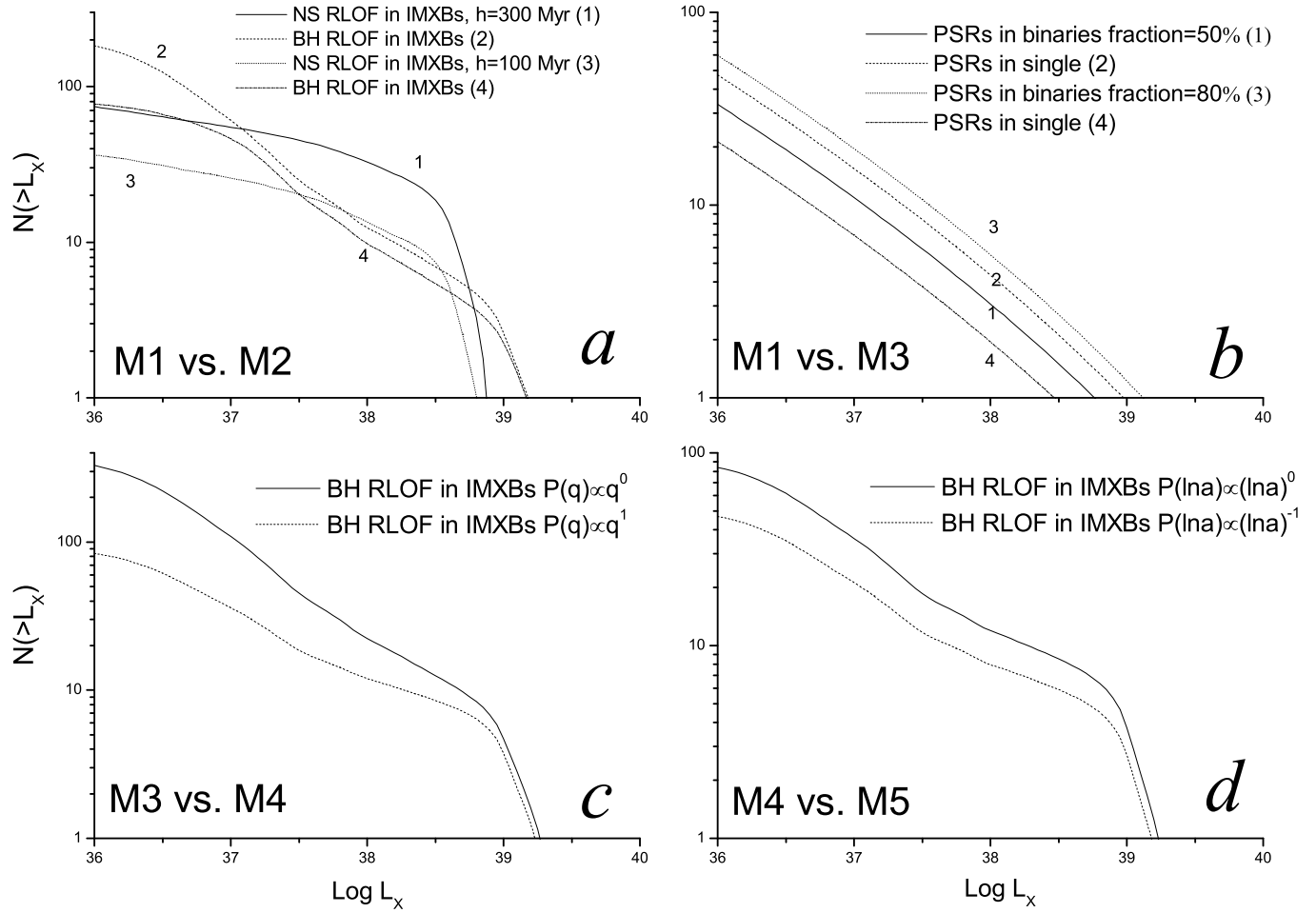


Fig. 3 Comparisons of the XLFs between various models. Panel (a): the NS & BH RLOF IMXBs are chosen to show the most prominent discrepancies between model M1 and M2; panel (b): comparison between model M1 and M3; panel (c): comparison between model M3 and M4; panel(d): comparison between model M4 and M5.

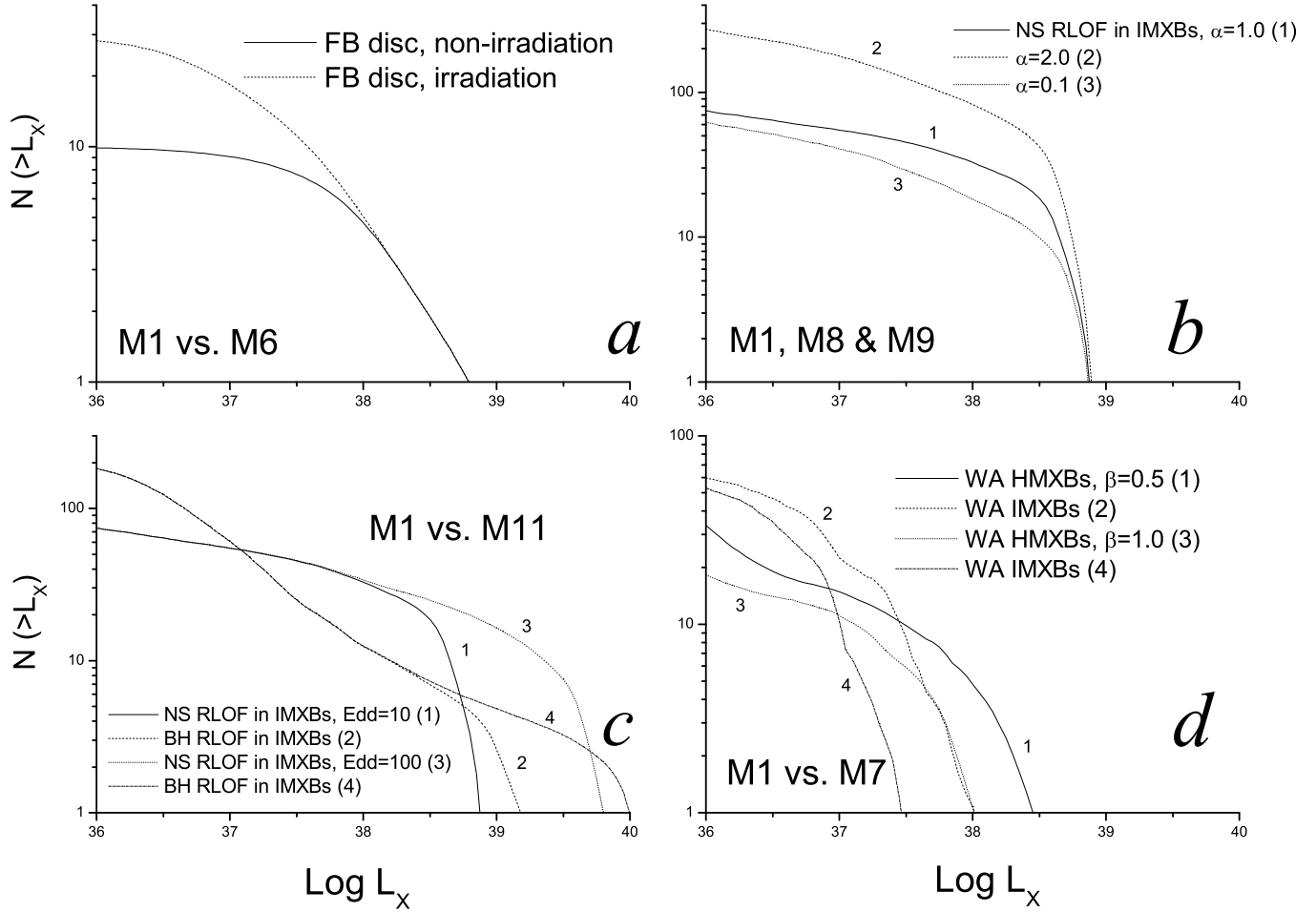


Fig. 4 Same as Fig.3. Panel (a): comparison of model M1 and M6 to show the effect of self X-ray irradiation on the fallback disc; panel (b): comparison between model M1, M8 and M9; panel (c): comparison between model M1 and M11; panel(d): comparison between model M1 and M7.

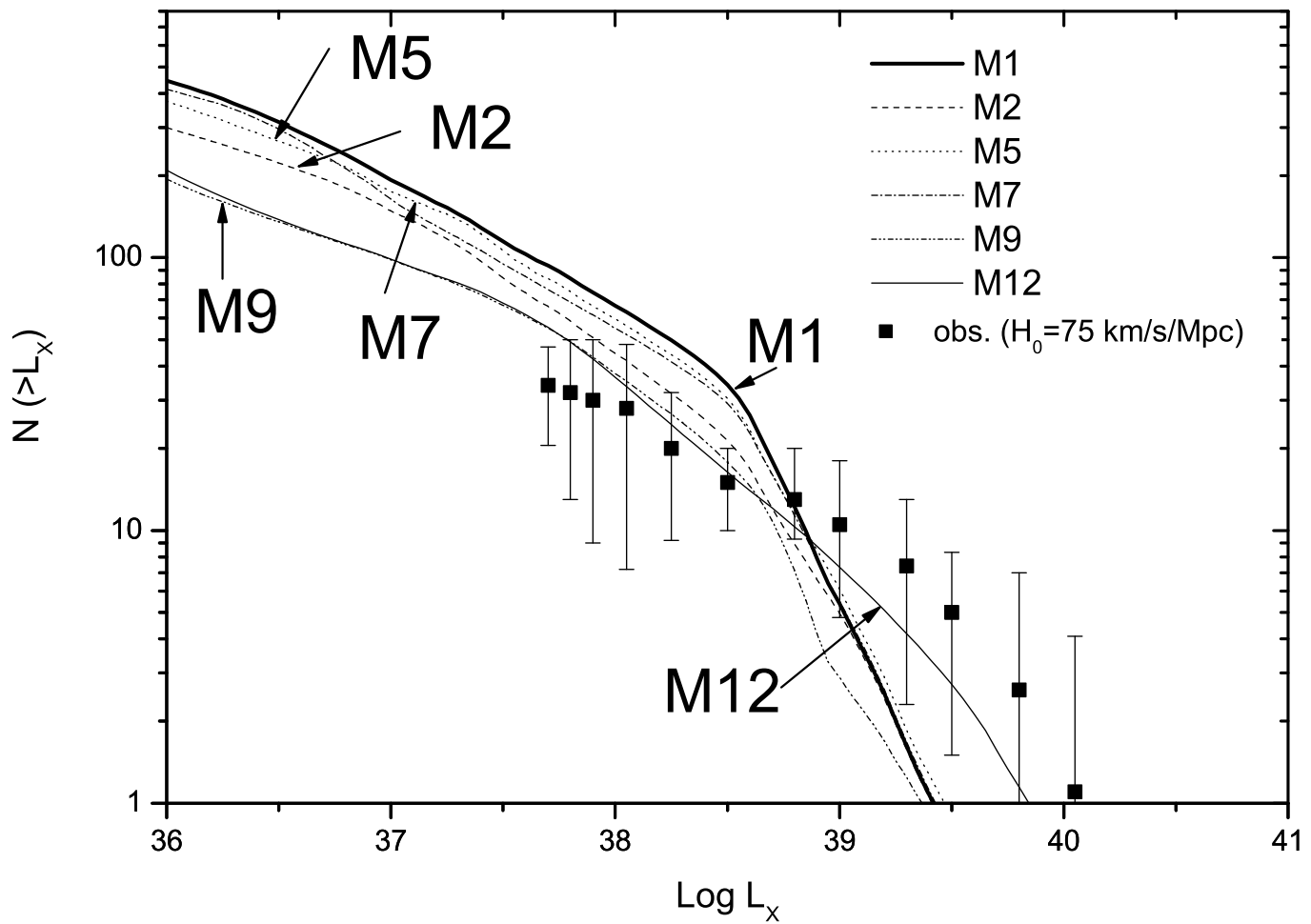


Fig. 5 The XLFs of six models M1, M2, M3, M5, M7 and M12, together with the observational data.

Table 1 Model parameters.

Model	α_{CE}	SFH ^a	f	$P(q)$	$P(\ln a)$	irradiation	β	Z	Edd ^b
M1	1.0	300	0.5	$\propto q^0$	$\propto (\ln a)^0$	no	0.5	0.02	10
M2	1.0	100	0.5	$\propto q^0$	$\propto (\ln a)^0$	no	0.5	0.02	10
M3	1.0	300	0.8	$\propto q^0$	$\propto (\ln a)^0$	no	0.5	0.02	10
M4	1.0	300	0.8	$\propto q^1$	$\propto (\ln a)^0$	no	0.5	0.02	10
M5	1.0	300	0.8	$\propto q^1$	$\propto (\ln a)^{-1}$	no	0.5	0.02	10
M6	1.0	300	0.5	$\propto q^0$	$\propto (\ln a)^0$	yes	0.5	0.02	10
M7	1.0	300	0.5	$\propto q^0$	$\propto (\ln a)^0$	no	1.0	0.02	10
M8	2.0	300	0.5	$\propto q^0$	$\propto (\ln a)^0$	no	0.5	0.02	10
M9	0.1	300	0.5	$\propto q^0$	$\propto (\ln a)^0$	no	0.5	0.02	10
M10	1.0	300	0.5	$\propto q^0$	$\propto (\ln a)^0$	no	0.5	0.001	10
M11	1.0	300	0.5	$\propto q^0$	$\propto (\ln a)^0$	no	0.5	0.02	100
M12	0.1	300	0.8	$\propto q^1$	$\propto (\ln a)^{-1}$	no	0.5	0.02	100

a: in units of Myr

b: the factor of super-Eddington accretion rate allowed